7680 *Macromolecules* **2010**, *43*, 7680–7688
DOI: 10.1021/ma101484e

Macromolecules
ARTICLE

Tensile Strength and Young's Modulus of Polyisoprene/Single-Wall Carbon Nanotube Composites Increased by High Pressure Cross-linking.

Bounphanh Tonpheng,[†] Junchun Yu,[†] Britt M Andersson,[‡] and Ove Andersson*,[†]

[†]*Department of Physics, Umea University, 901 87 Umea, Sweden, and* [‡]*Department of Applied Physics and Electronics, Umea University, 901 87 Umea, Sweden*

Received July 3, 2010; Revised Manuscript Received August 9, 2010

ABSTRACT: High-viscosity liquid *cis*-1,4 polyisoprene (PI), with up to 20 wt % single-wall carbon nanotubes (SWCNTs), has been cross-linked by high pressure and high temperature (HP&HT) treatment at 513 K and pressures in the range 0.5 to 1.5 GPa to yield densified network polymer composites. A composite with 5 wt % SWCNTs showed 2.2 times higher tensile strength σ_{UTS} (σ_{UTS} = 17 MPa), 2.3 times higher Young's modulus E (E = 220 MPa) and longer extension at break than pure PI. The improvement is attributed to SWCNT reinforcement and improved SWCNT−PI interfacial contact as a result of the HP&HT cross-linking process, and reduced brittleness despite a higher measured cross-link density than that of pure PI. The latter may originate from an effect similar to crazing, i.e., bridging of microcracks by polymer fibrils. We surmise that the higher cross-link densities of the composites are due mainly to physical cross-links/constraints caused by the SWCNT−PI interaction, which also reflects the improved interfacial contact, and that the CNTs promote material flow by disrupting an otherwise chemically cross-linked network. We also deduce that the PI density increase at HP&HT cross-linking is augmented by the presence of CNTs.

Introduction

The use of composite materials that consist of materials with complementary properties has become a progressively more important tool in the development of advanced products. In particular, composites improve the possibilities of producing lightweight strong structures and materials with enhanced electrical and thermal properties. In this context, nanoscale fillers are especially interesting since these have a strong potential for inducing significant changes in properties even at low concentrations. As examples, carbon blacks, silicas, clays, and carbon nanofibers have been used to improve mechanical, electrical, and thermal properties of polymers.[1] More recently, carbon nanotubes (CNTs)[2] have been frequently tested as fillers to improve the properties of various matrix materials, which typically are polymers.[1] The CNT's unique combination of properties, such as high strength, low mass density, and high thermal and electrical conductivities, are excellent for making novel composites. Moreover, since the volume fraction needed for (geometrical) percolation decreases strongly with increasing aspect ratio (length/diameter),[3] this favors fillers of a one-dimensional nature. Thus, CNTs with aspect ratios that are typically $\sim 10^2$ and higher can have a significant impact on properties at minute concentrations, especially on transport properties, which strongly benefits from percolation when the filler has much higher conductance than the matrix. Another consequence of high aspect ratio, and therefore high specific surface area, is a more efficient load transfer between the matrix and filler. As long as the filler is sufficiently strong, then an increase of aspect ratio is also beneficial for improving the mechanical strength of a composite material. Many attempts to take advantage of CNT's properties in composites have focused on mechanical reinforcement of polymers, which is also the subject of this study, but the potential for CNT applications are numerous.[4−9]

*Corresponding author. E-mail: ove.andersson@physics.umu.se.

There are two main types of CNTs: single-wall carbon nanotubes (SWCNTs) and multiwall carbon nanotubes (MWCNTs). A SWCNT can be described as a (2D) graphene sheet rolled up into a cylinder, which may be capped at the ends by hemispheres of the buckyball structure. The sp^2 hybridized carbon atoms in graphene get slight sp^3 character in the cylindrical form, and this tendency increases as the radius of the cylinder decreases. The diameters of the SWCNTs are in the range 0.7−10.0 nm but are normally less than 2 nm,[10] and the length is on the order of micrometers. MWCNTs consist of an array of cylinders formed concentrically around a central hollow core with interlayer separations of ∼0.34 nm,[11] which is the same as for the graphene layer spacing of graphite.

In 1993, Overney et al.[12] used computer calculations to investigate rigidity and low-frequency vibrational properties of CNTs. Their results for bending of a carbon nanotube with 200 carbon atoms, which was clamped on one side and free on the other, may be converted to give a Young's modulus of ∼1.5 TPa, and a more recent study reported a modulus of 1.0 TPa.[13] These are about the same or only slightly larger than 1.1 TPa found in the basal plane, or the graphene layers, of graphite,[14] 0.5 TPa for suspended graphene sheets,[15] and ∼1.1 TPa for diamond.[16] Subsequent experimental investigations have yielded results that are in fair agreement with the predictions. Yu et al.[17] measured force−strain data for SWCNT ropes and deduced that a model in which the load was carried only by the SWCNTs on the perimeter of the rope best fitted the experimental results. On the basis of this model, they reported Young's modulus values for SWCNTs in the range 0.32−1.47 TPa, with a mean of 1.00 TPa. Moreover, the same model yielded tensile strengths in the range 13−52 GPa.

The Young's modulus for polymers can be as large as 3.5 GPa,[18] but is normally much lower and especially for elastomers, e.g. that of sulfur vulcanized polyisoprene (PI) is typically 1−2 MPa,[19,20] with a tensile strength 17−25 MPa.[20] Thus, considering the large values for CNTs, there is a great potential for reinforcement of polymer matrixes by inclusion of CNTs, and the progress

 Published on Web 08/17/2010

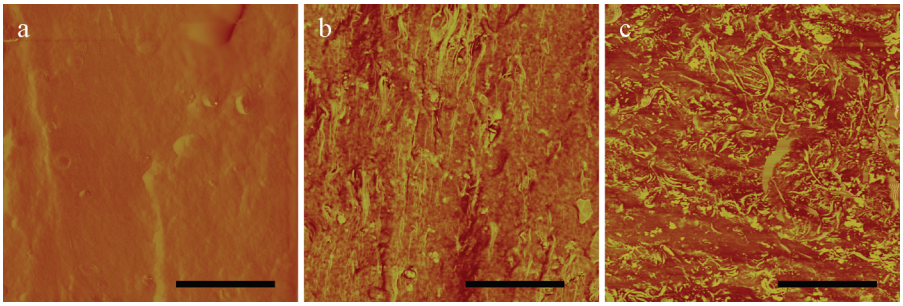

Figure 1. AFM phase images of the sample surface after treatment for 4 h at 1 GPa and 513 K: (a) pure PI, (b) PI with 3 wt % SWCNTs, and (c) 10 wt % SWCNTs, respectively. The scale bar is 1 μm.

has recently been reviewed.[21,22] One significant problem is the normally weak interfacial interaction between the matrix and the CNTs, which limits the transfer of load to the high-strength CNTs. To achieve substantial reinforcement it is therefore crucial to find ways to improve the interfacial interaction or else the CNTs will simply be pulled out of the matrix. Recent interesting attempts have employed functionalized CNTs, which can both improve the dispersion of the CNTs, and provide a site for obtaining strong bonds and/or entanglement between the CNTs and the matrix.[7] In this work, we investigate the effect of another method, which improves the interfacial contact via cross-links induced under densified conditions.

Here we present the first comprehensive study of the tensile properties for CNT polymer composites synthesized by high pressure high temperature (HP&HT) cross-linking. It has been previously shown that HP&HT treatment can be used to cross-link polymers such as poly(butadiene) and copolymers of poly(butadiene) and acrylonitrile (nitrile rubber).[23] More recently, it was reported that tetraethylene glycol dimethacrylate can be both polymerized and cross-linked under pressure.[24] Moreover, we have established that PI can be cross-linked into a densified elastomeric state purely by HP&HT treatment.[25,26] Since vulcanization systems are omitted, their effect on polymer matrix and polymer composite properties is also excluded, which can be beneficial for studying CNT induced effects in composites and provide further insight into CNT−polymer interfacial interactions. We have here used a similar recipe as that established for pure PI to obtain well cross-linked and densified PI−SWCNT composites via HP&HT treatment for studies of their tensile properties. We show that SWCNTs in highly cross-linked and densified PI both provide reinforcement and reduce the brittleness of the polymer matrix, which we attribute to a CNT promoted phenomenon similar to crazing.[27]

Experimental Section

Materials. SWCNTs produced by the electric arc-discharge technique with a metal content in the range of 7−10 wt % and a carbonaceous purity of 70−90% were purchased from Carbon Solution Inc. The average diameter of the SWCNT was 1.4 nm, and the lengths were in the range 0.5−1.5 μm in bundles of 4−5 nm in diameter. Since this was the bundle size before the long and strong sonication in both toluene and toluene−PI solution (see below), it should provide an upper limit of the bundle size. Liquid *cis*-1,4-poly(isoprene) made from natural rubber, with a number-average relative molecular mass of 38 000, was purchased from Sigma- Aldrich.

Preparation of Composites. Composites were prepared by sonication of SWCNTs or carbon black (CB) (N550: particle size 40−48 nm, surface area 40−49 $m^2\ g^{-1}$) and PI in toluene. The method has been used before in a study of the thermal properties of PI−SWCNT composites.[26] Briefly, a mixture of SWCNTs and toluene in a glass beaker, sealed partly by Al foil, was sonicated using a 130 W, 20 kHz ultrasonic processor (VCX130, Sonics & Materials, Inc. USA) at room temperature for 1 h, using 75% of full power. Simultaneously, PI was mixed in toluene using a magnetic stirrer until it was uniformly dissolved, and then added to the SWCNT−toluene mixture. Thereafter, the sonication of the mixture was continued using 50% of full power, with the Al foil removed, which caused the toluene to slowly evaporate and the mixture became progressively more viscous. The viscous mixture was dried for several days under dynamic vacuum at 70 °C to remove the remaining toluene.

A PI−CB composite was prepared by mixing CB and PI, respectively, in toluene using a magnetic stirrer until it was uniformly dissolved, whereafter the two mixtures were combined. Subsequently, the PI−CB-toluene mixture was sonicated using the ultrasonic processor until it became highly viscous. Finally, the high-viscosity mixture was continuously dried for several days under dynamic vacuum to remove the remaining toluene.

Experimental Procedure for High Pressure High Temperature Treatment of Samples. The samples (PI, PI−SWCNTs or PI−CB composite) were loaded into Teflon cells, which fitted in a piston-cylinder device of 45 mm internal diameter, and transferred to a hydraulic press. The samples were pressurized at room temperature with a rate ~0.3 GPa h^{-1} up to a pressure in the 0.25 to 1.5 GPa range. (Samples in the 0.25 to 0.4 GPa range were only used to establish the pressure dependence of the cross-link density.) The pressure settings were determined from load/area, with an empirical correction for friction, which had been established using the pressure dependence of the resistance of a Manganin wire. The maximum inaccuracy in pressure was estimated as ±40 MPa at 1 GPa. Subsequently, the samples were heated isobarically from room temperature to 513 K at a rate of 0.5 K/min and annealed for 4 h at 513 K, by means of an external heater that surrounded the vessel. This temperature has been previously established as suitable, i.e. it yields an appropriate cross-linking density, for studies in the pressure range 0.5−1.5 GPa.[25] The temperature of the sample was measured using an internal Chromel Alumel thermocouple with an estimated inaccuracy of ~0.2 K. However, the temperature gradient in the samples, which were 39 mm in diameter and ~2 mm thick, probably exceeded this value during the cross-link process at 513 K. Although, the temperature was regulated using a proportional−integral−derivative controller, the temperature sometimes fluctuated about ±1 K during the 4 h anneal. As discussed below, both pressure and temperature variations may be one cause for the observed differences in the cross-link density for samples with nominally identical treatment. After annealing, the temperature was first decreased to room temperature and then the pressure lowered to atmospheric pressure. Figure 1 shows surface images of the recovered samples and the achieved dispersion of the CNTs in PI after the high pressure treatment. These phase images were measured by tapping-mode atomic force microscopy (AFM) (Nanoscope IV Controller, Veeco Metrology) on sections that had been cut using a Leitz microtome after freezing the samples in liquid nitrogen.

Characterization of Cross-Link Density, Mass Density, and Mechanical Properties after High Pressure High Temperature Treatment. Cross-link density was determined using the swelling method. The samples were swelled in *n*-heptane at room temperature until the swelling reached equilibrium which took approximately 48 h, and the cross-link densities were calculated by the Flory−Rehner equation,[28,29] which has been previously described in detail.[26] A composite with 10 wt % SWCNT, as well as a sample of pure PI, were swelled for twice as long time, i.e., 96 h, to ensure that the higher cross-link densities measured for the composites were not due a longer time to reach equilibrium. Moreover, a few of the pure samples and composites were swelled also in toluene to verify that the measured reduced swelling of the composites was not specific for n−heptane. In the case of toluene, the polymer−solvent interaction parameter χ was calculated from $\chi = 0.427 + 0.112\phi^2$,[30] where ϕ is the PI volume fraction in the swelled sample. The measured cross-linking densities using toluene were typically roughly 50% lower than those using *n*-heptane, but both showed qualitatively the same dependence on CNT content and high temperature high pressure treatment.

Tensile testing of the pure PI, PI−CB, and PI−SWCNT composites were performed using an Instron 3343 with a 500 N-load cell at room temperature with a testing speed of 10 mm/min. The tensile samples were cut from the high pressure produced plate-shaped samples using a custom-made dogbone-shaped die yielding 16 mm long, 7 mm wide, and ~2 mm thick pieces. The exact dimensions were measured by means of a workshop microscope, and these (initial) values were used in the calculations of the tensile stress and Young's modulus (in the range 1−5% strain). To ensure accuracy and repeatability, at least two test pieces from the same sample were tested.

Scanning electron microscope images (Philips ESEM XL30) of pure PI and 5, 10, and 20 wt % PI−SWCNT composites, which had been cross-linked at 1 GPa, were taken after tensile testing.

Mass density was measured by the Archimedes' principle by immersing in water as well as by submerging in various methanol/water mixtures kept at 25 °C with an estimated inaccuracy of ±0.5%.

Results and Discussion

Effect of Treatment Pressure on Tensile Properties of Polyisoprene. Tensile stress−extension curves of high-pressure high-temperature (HP&HT) treated PI are shown in Figure 2. The samples were prepared by pressurizing virgin (liquid) PI at room temperature to 0.5 GPa or higher (see Experimental Section) and subsequent heating to 513 K, where the samples were annealed for 4 h. This treatment induces cross-links and transforms liquid PI into an elastomeric state, or a network polymer.[25,31]

The shape of the stress−extension curves changes gradually with increasing treatment pressure from that typical of an elastomer toward that of a brittle polymer, with a decreasing slope with increasing extension. Moreover, the results show that the (ultimate) tensile strength σ_{UTS} and the Young's modulus E improve while the extension at brake decreases. The pressure induced improvement of σ_{UTS} appears moderate up to 0.8 GPa but substantial, 150−270%, between 0.8 and 1 GPa, and σ_{UTS} increases further by 650% between 1 and 1.5 GPa (Figure 3a). The Young's modulus follows a similar trend and increases 340−800%, between 0.8 and 1 GPa, and by as much as ~2000% between 1 and 1.5 GPa (Figure 3b). These changes in the tensile properties for the samples occur in parallel of a pressure induced increase of the cross-link density. As shown in Figure 3c, the cross-link density increases almost logarithmically with treatment pressure, which accounts for the improvement of σ_{UTS} and

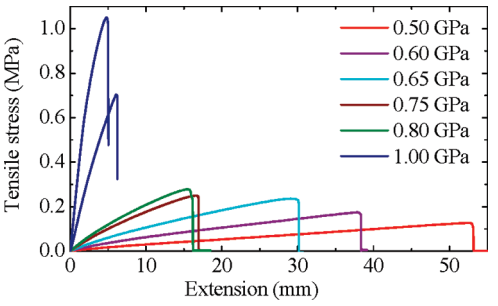

Figure 2. Tensile stress plotted against extension for pure PI treated 4 h at 513 K and 0.5, 0.6, 0.65, 0.75, 0.8, and 1.0 GPa (two different batches), respectively.

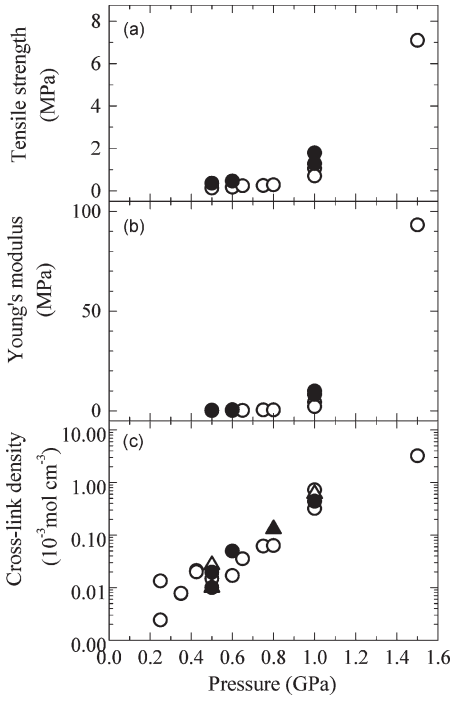

Figure 3. (a) Tensile strength and (b) Young's modulus plotted against the pressure of the HP&HT treatment: (○) PI and (●) PI−SWCNT with 1 wt % CNTs. (c) Cross-link density plotted against the pressure of the HP&HT treatment: (○) PI (△ data from ref 26) and (●) PI−SWCNT with 1 wt % CNTs (▲ data from ref 33).

E. However, although the increasing number of carbon−carbon links between the chains improves the strength, the samples become progressively more brittle and therefore more difficult to handle.[32]

The results in Figure 3c show that nominally the same treatment for two samples can yield a significant difference in cross-link density and, as shown by the results for two different 1 GPa treated samples (Figure 2), this is also reflected in their tensile properties. Although the temperature is measured in situ, we surmise that temperature and/or pressure differences, which may be caused by gradients in the 39 mm in diameter and 2 mm thick samples, can alter the cross-linking rates during the 4 h HP&HT treatments. Measurements on mm-sized pieces taken from various places of one HP&HT produced plate yielded values of the cross-link density that differed up to 25% whereas the scatter in repeated measurements on one piece was less than 8%. The tensile strength results for two tensile samples cut from the same plate could differ up to 12%.

The changes of both σ_{UTS} and E, shown in Figure 3, panels a and b, are reminiscent of exponential increases with

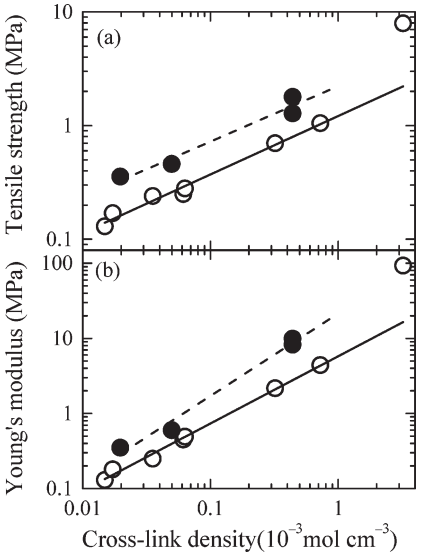

Figure 4. (a) Tensile strength, and (b) Young's modulus plotted against cross-link density for: (○) PI and (●) PI−SWCNT with 1 wt % CNTs for samples treated in the 0.5−1.5 GPa range at 513 K. The lines represent fits (see text).

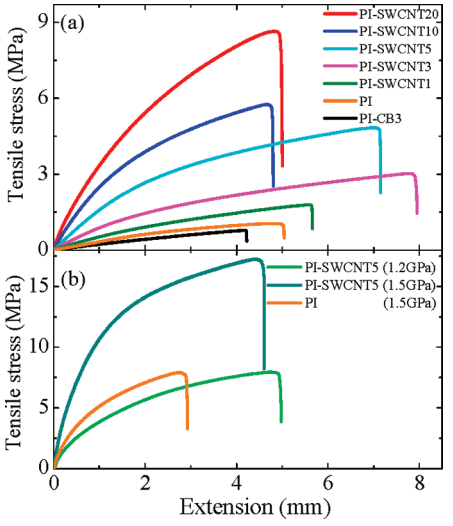

Figure 5. (a) Tensile stress plotted against extension for PI, PI−SWCNT and PI−CB composites treated 4 h at 513 K and 1 GPa. (b) Tensile stress plotted against extension for PI and 5 wt % PI−SWCNT composites treated 4 h at 513 K and 1.2 or 1.5 GPa.

increasing pressure, i.e., the same as for the cross-link density. Thus, it is reasonable to attribute the increases of σ_{UTS} and E to the change in the cross-link density, and such dependences are supported by the plots in Figure 4. In logarithmic plots, both σ_{UTS} and E change roughly linearly against the cross-link density, at least up to moderately high cross-link densities (below 10^{-3} mol cm^{-3}). In this range, a fit of $E \sim v^x$, where v is the cross-link density and x is a fitting parameter, yielded $x = 0.9$. This is close to $E \sim v$, which has been observed by changing the cross-link density through radiation treatments.[34] The corresponding fit for σ_{UTS} yielded $x = 0.51$.

The logarithmic increase of the cross-link density with pressure of the HP&HT treatments shows that the cross-linking rate is volume dependent. That is, the reduced volume and consequential decrease of distance between the polymer chains increases strongly the probability of the process. In fact, it becomes vanishingly small at atmospheric pressure and must be accelerated by vulcanization chemicals to obtain an elastomeric state. As shown below, the cross-linked states formed by the HP&HT treatment have higher mass density, or lower specific volume, than the virgin state.[35] This volume decrease between the initial and final state lowers the energy of the system and provides a driving force for the cross-link process.

As discussed before,[25] the cross-link process in PI may proceed in a similar manner as that suggested for poly(butadiene), which exhibits even higher cross-link rate than PI at the same HP&HT conditions. The HP&HT induced cross-linking of poly(butadiene) has been attributed to a (secondary allylic) radical process, similar to that in peroxide and radiation cross-linking, which propagates through an efficient addition mechanism that consumes mainly pendant vinyl unsaturations.[23,36,37] The more stable tertiary allylic radical, which may form in PI, does not easily undergo cross-linking with other radicals or neighboring chain double bonds,[38] which explains the lower cross-linking rate of PI.

Effects of Treatment Pressure and CNTs on Tensile Properties of PI−SWCNT Composites. The effect of treatment pressure on the tensile properties of PI−SWCNT composites, with 1 wt % SWCNTs, were studied for samples which had been cross-linked at 0.5, 0.6, and 1.0 GPa, respectively. The results are shown in Figure 3a and 3b and, as for pure PI, both σ_{UTS} and E increase strongly with treatment pressure. Moreover, logarithmic plots of σ_{UTS} and E against cross-link density show that those of the composite exhibit about the same cross-link dependency below $\sim 10^{-3}$ mol cm^{-3} as pure PI (Figure 4). A fit of $E \sim v^x$ yielded $x = 1.1$, i.e., somewhat larger than that for pure PI. The corresponding fit for σ_{UTS} yielded $x = 0.49$, which is the same as that for pure PI.

At cross-link densities below $\sim 5 \times 10^{-4}$ mol cm^{-3}, i.e., for samples cross-linked below 1 GPa, addition of 1 wt % CNTs decreased the extension at break,[33] whereas it increased the extension for the highly cross-linked 1 GPa treated samples (Figure 5a). Since the CNT content of the composite remained the same and the only major change in the samples is that of the cross-link density, this crossover in behavior must be associated with the increase in cross-link density. As the (chemical) cross-link density increases with increasing pressure for the HP&HT treatment, the plastic and elastic extensions of PI becomes limited, and the tensile stress−extension curves change from elastic to brittle-like behavior, as shown in Figure 2. It thus seems reasonable to attribute the longer extension of the composites to a CNT caused disruption of the highly cross-linked PI networks that form at 1 GPa and above. The lack of such noticeable features at low cross-link densities is then a natural consequence of the much smaller number of cross-links in a volume occupied by a CNT. The crossover from a CNT induced decrease of the extension to a CNT promoted increase occurs when the cross-link density increases from 10^{-5} to 10^{-3} mol cm^{-3} (Figure 3c). For CNTs of 1.4 nm in diameter and 1 μm long, this corresponds to a change from 10 to 10^3 cross-links per CNT volume, and for CNT bundles of 4−5 nm in diameter, i.e., the size of the as-purchased material, these numbers increase by a factor of 10.

Another set of composites was produced under nominally identical HP&HT conditions by annealing for 4 h at 1 GPa and 513 K. The complete set of PI−SWCNT composites included 1, 3, 5, 10 (2 batches), and 20 wt % CNTs, which are labeled PI−SWCNT1, PI−SWCNT3, PI−SWCNT5, and PI−SWCNT10, and PI−SWCNT20 respectively. Moreover, a composite with 3 wt % carbon black (N550), labeled PI−CB3, was made for comparison. The two batches of 10 wt % SWCNT each yielded two tensile samples. (Only one

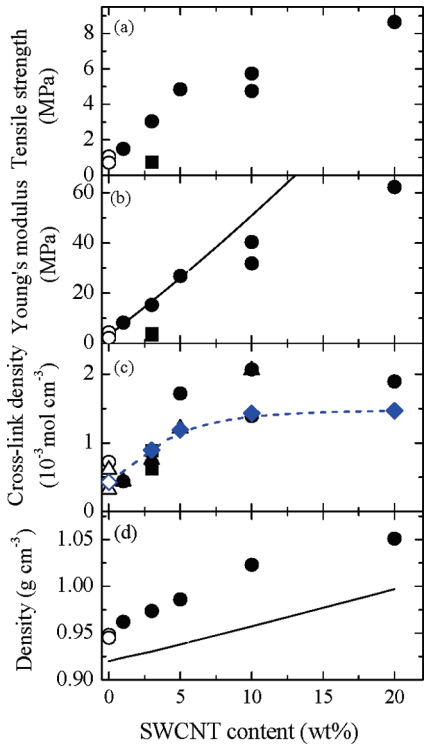

Figure 6. (a) Tensile strength and (b) Young's modulus plotted against filler content for: (○) PI, (●) PI−SWCNT and (■) PI−CB. The line shows Young's modulus calculated by eq 3 assuming an aspect ratio of 500. (c) Cross-link density plotted against filler content for: (○) (△)[26] PI, (●) (▲)[26] PI−SWCNT, and (■) PI−CB. (◇, ◆, in blue) connected by the dashed line shows results by swelling in toluene instead of *n*-heptane (see Experimental Section). (d) Density plotted against CNT content for (○) PI, and (●) PI−SWCNT. The line in panel d shows densities calculated from the mixture rule (eq 5) based on values stated for as-purchased (untreated) PI and SWCNTs. All samples were cross-linked by treatment for 4 h at 1 GPa and 513 K.

of the four tensile tests is shown in Figure 5.) The σ_{UTS} and E of the two samples agreed to within 5 and 20% respectively. The corresponding differences between the two batches were 24% and 33%, which is partly explained by a difference in cross-link density.

The tensile stress−extension curves of the composites, together with that for pure PI, are shown in Figure 5a, and the tensile properties are summarized in Figure 6, which shows average values of at least two tests. The shapes of the curves of the PI−SWCNT composites are similar and brittle-like with a significantly decreasing slope. The tensile strengths of the PI−SWCNT composites were 70%, 190%, 360%, 450% (350%), and 720% larger than that of PI for 1, 3, 5, 10, and 20 wt % CNT content, respectively, whereas the PI−CB3 composite was slightly weaker.

In an ultimate test, three samples were made also at 1.2 and 1.5 GPa:[32] two 5 wt % composites and one pure PI (Figure 5b). The HP&HT cross-linking of pure PI at 1.5 GPa increased its σ_{UTS} and E to as much as 7.9 and 93 MPa, respectively. The corresponding values for the 5 wt % composite were σ_{UTS} = 17.3 MPa and E = 220 MPa. Consequently, the composite was 2.2 times stronger and had 2.3 times higher Young's modulus than pure PI. But the corresponding fractional increases for σ_{UTS} and E of the 1 GPa HP&HT treated 5 wt % composite were even larger: 5 and 8 times, respectively.

Besides the SWCNT reinforcement of PI, Figure 5a shows that increasing SWCNTs content up to a certain degree also further improves the extension at break for the samples produced at 1 GPa, i.e. these composites display an augmented behavior discussed above for the 1 wt % composites. More specifically, increasing amount of SWCNTs up to about 3 wt % improves the extension at break, whereas it decreases on additional increase of SWCNT content and finally becomes the same as for pure PI. Thus, in the range up to ~3 wt % SWCNTs, the extension at break may improve by the CNT disruption of the network in PI and the consequentially improved plastic flow and elastic extension. However, at further increase of SWCNTs, the low flexibility of these also becomes a limiting factor for the extension of the composites. This feature of a maximum in the extension at break against CNT content may occur in other types of polymers as well, i.e. also those without chemical cross-links, as long as the CNTs promote plastic flow. The CNT induced disruption of the PI network and the increased mass density of the composites (Figure 6d) are discussed in more detail below.

The CNT filler provides reinforcement for PI but, as shown in Figure 6, panels a and b, the increase of σ_{UTS} and E levels off, which suggests that the dispersion deteriorates at high CNT content. Another indication of this is provided by the change of cross-link density with filler content, shown in Figure 6c. The data show that the cross-link density is enhanced by the carbon fillers and also that this effect levels off at high filler content.[39] The results of the swelling method, which was used to determine the cross-link density, include both chemical and physical cross-links that limit the swelling. The latter is normally associated with (trapped) entanglements but also other physical constraints for the polymer chains, e.g., those caused at the interface between filler and polymer, would be reflected in swelling results, which has been recently discussed in detail.[40] The polymer conformation at the interface between PI and the CNTs is not known but both experimental results and simulations have indicated that polymer wrapping of CNTs can be energetically favorable, which is one possibility for physical constraints.[41,42] Thus, if the filler provides physical (and chemical) constraints for the polymer chains, the increase of cross-link density measured by the swelling method would level off if the dispersion deteriorates at high CNT content, which is in agreement with the observed results.

Another interesting result is the lack of improvement of σ_{UTS} for the PI−CB3 composite. Carbon black is known to provide strong reinforcement at high loadings but despite that the cross-link density increases by the inclusion of 3 wt % CB, σ_{UTS} and E slightly decrease (Figure 6, panels a and b). This shows that the increase of cross-link density cannot be due to more (chemical) cross-links in the PI network, which would increase σ_{UTS} and E. This also suggests that the increase of cross-link density for the PI−SWCNT composites is unlikely due to an increase of cross-link density in the PI network. In fact, the results for the improved extension of the PI−SWCNT composites discussed above are in correspondence with a *decrease* of cross-links in the PI network. The increase of cross-link density with CNT/carbon content may instead be due to physical cross-links/constraints caused by the interface between the carbon filler and the matrix. This conclusion is corroborated by a detailed study of the nature of cross-links in natural rubber-functionalized graphene nanocomposites by Valentín et al.[40] Considering that a CNT is basically a graphene sheet rolled up into a cylinder, their results should be applicable on this study. Valentín et al.[40] showed that the cross-link density obtained via swelling measurements was significantly larger than that observed in NMR results. The latter indicated that the cross-link density of the matrix was "unaffected or even

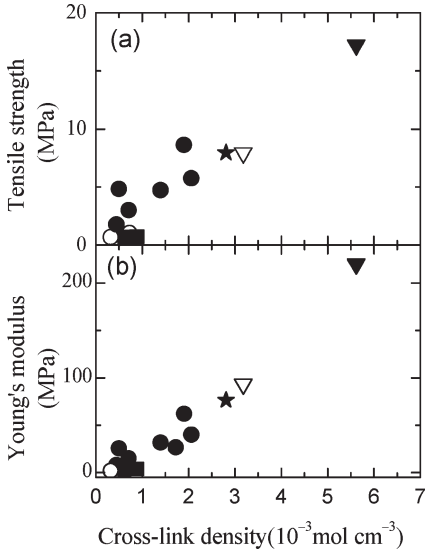

Figure 7. (a) The tensile strength plotted against cross-link density for (○, ▽) PI, (●, ★, ▼) PI−SWCNT, and (■) PI−CB3. (b) Young's modulus plotted against cross-link density for (○, ▽) PI, (●, ★, ▼) PI−SWCNT, and (■) PI−CB3. The samples were cross-linked by treatment for 4 h at 513 K and 1 GPa (circles and squares), 1.2 GPa (stars), and 1.5 GPa (triangles).

deteriorated". Valentín et al.[40] attributed the reduced swelling of the composite to the "interface material" and concluded that such an effect occurs in composites with "strong rubber−filler interaction". Specifically for graphene, they noted that "in the swollen state the material properties are completely dominated by the interface behavior, revealing a significant nanoeffect".

Although SWCNTs have larger specific surface area than CB, which may assist the formation of physical cross-links/constraints, the single result for CB indicates that it increases the cross-link density to about the same extent as SWCNTs. However, CB does not improve the tensile properties as done by the SWCNTs. Thus, the large aspect ratio and high strength of CNTs make a significant difference for the purpose of achieving reinforcement. It follows that the interfacial interaction between CB/SWCNT and PI is about equally reflected in the measured cross-link density but it leads to significantly different changes in σ_{UTS} and E due to the much weaker reinforcement by CB in comparison to that by CNTs.

Figure 7 shows σ_{UTS} and E versus cross-link density for composites with varying CNT content and pressure treatments, and the corresponding results for pure PI and PI with 3 wt % carbon black. Despite that the CNT content differs in the PI−SWCNT composites, E (and σ_{UTS}) increases roughly linearly with the measured cross-link densities. It follows that the cross-link density measured by the swelling method is an indicator of the reinforcement of the composite, i.e. the same as for pure PI (Figures 4 and 7). In the case of pure PI, the explanation for this dependence is straightforward as more carbon−carbon cross-links make the matrix stiffer and stronger. For the PI−SWCNT composites, which generally show higher cross-link densities than PI for the same HP&HT treatment, the increase of σ_{UTS} and E cannot be due to more carbon−carbon cross-links in the PI matrix. As discussed above, this would make the matrix more brittle, whereas the results show the reverse. The change is instead attributable to improved CNT−PI interfacial interaction and CNT reinforcement, which increases with improved load transfer. The concomitant increase of cross-link density would thus be partly a reflection of this increased CNT−PI interfacial interaction. The measured cross-link density increases with both increasing CNT content and increasing pressure for the HP&HT treatment. The increase with CNT content should be due to the increase of the CNT surface area, whereas the pressure induced increase is likely due to a combined effect of improved interfacial interaction (see calculations below) and an increased number of carbon−carbon cross-links in the PI matrix, despite that the latter is partly suppressed by the presence of CNTs. This disruption of the PI network by the CNTs, which is indicated by the longer extension at break for highly cross-linked PI, may occur also in the PI−CB3 composite. Since the CB does not provide the same reinforcement as CNTs this may explain the slight decreases of σ_{UTS} and E. We can also conclude that the (linear) increase of σ_{UTS} and E with increasing cross-link density for the PI−SWCNT composites corroborates the results of the swelling measurements. That is, since the measured CNT induced increase of cross-links also yields an increase of the tensile properties, it seems to be a real effect and not anomalous due to some other effect that reduces the swelling, e.g., increased time to reach equilibrium.

Models for the Tensile Strength and Young's Modulus. To quantitatively evaluate the deductions made above, we can use the most commonly employed models for filler induced reinforcement. A theoretical estimate of the maximum tensile strength of the composites, valid for long aligned fibers, is provided by[21,43]

$$\sigma_{composite} = \sigma_{CNT}\,\phi_{CNT} + \sigma_{PI}\,\phi_{PI} \quad (1)$$

where $\sigma_{composite}$, σ_{CNT}, σ_{PI} are the tensile strength of the composite, SWCNTs (~30 GPa)[4] and PI matrix, respectively, and ϕ is the volume fraction. The tensile strength for the PI matrix was taken from the results for PI cross-linked at 1 GPa (σ_{PI} = 1 MPa). This estimate gives a value for σ_{UTS} of the composite of about 0.6 GPa for a 3 wt % (~2 vol %) PI−SWCNT composite. The large difference (~200 times) between this theoretical estimate and the experimental results indicate that the interfacial stress transfer between the PI matrix and the SWCNTs is insufficient to obtain maximum reinforcement. Although random orientation and bundling of the SWCNTs also account for a significant part of the difference, these effects seem unable to explain all the difference unless the bundle size increases significantly from the stated value of 4−5 nm of the as-purchased SWCNTs. It follows that the failure mechanism of the composites is likely due to CNT pull-out.

In the case of CNT pull-out, σ_{UTS} of the composites is described by[21]

$$\sigma_{composite} = \frac{\tau l_{CNT}}{d_{CNT}}\,\phi_{CNT} + \sigma_{PI}\phi_{PI} \quad (2)$$

where τ is the interfacial stress transfer between the CNTs and PI, l_{CNT} (~1000 nm), and d_{CNT} (1.4 nm) are the CNT's length and diameter, respectively. Even though the magnitude of τ obtained from eq 2 may be too small because of SWCNT bundling (about a factor of 5 for a bundle diameter of 5 nm), it can be used to determine the change of τ with different HP&HT treatments. The calculations of τ for HP&HT treatments at 0.5 GPa (1 wt % SWCNTs),[33] 1 GPa (1 and 5 wt % SWCNTs) and 1.5 GPa (5 wt % SWCNTs), yield 0.04, 0.16, and 0.4 MPa. The two values of τ for different CNT contents at 1 GPa were in good agreement, 0.15 and 0.16 MPa for 1 and 5 wt % CNTs, respectively, despite that bundling is likely somewhat more pronounced

for composites with higher CNT content. Thus, the values are reliable and imply that the interfacial stress transfer increases significantly with increasing pressure of the HP&HT cross-link process.

There are several equations used to predict the Young's modulus for a composite and various forms of the Halpin−Tsai model[44−46] are commonly employed. In this case we use a simplified form derived for randomly oriented fibers, which we believe provides the best approximation for the composites. Visual analysis of AFM-images of the sample, which had been taken in the direction of the applied load and perpendicular to this direction, supports that the CNTs are randomly oriented in three dimensions. In this form of the Halpin−Tsai model, the composite modulus $E_{composite}$ is given by[44,46]

$$\frac{E_{composite}}{E_{PI}} = \frac{1}{5}\left[\frac{1+2p\eta_L\phi}{1-\eta_L\phi}\right] + \frac{4}{5}\left[\frac{1+2\eta_T\phi}{1-\eta_T\phi}\right] \quad (3)$$

where

$$\eta_L = \frac{E_{\mathrm{CNT}}/E_{PI} - 1}{E_{\mathrm{CNT}}/E_{PI} + 2p}$$

and

$$\eta_T = \frac{E_{\mathrm{CNT}}/E_{PI} - 1}{E_{\mathrm{CNT}}/E_{PI} + 2}$$

E_{CNT} and E_{PI} are the Young's moduli of the SWCNTs and PI (3.3 MPa), respectively, ϕ is the volume fraction, p is the aspect ratio, i.e. the ratio between the CNT's length and diameter ($= l_{\mathrm{CNT}}/d_{\mathrm{CNT}} =$ 1000 nm/1.4 nm).

The following relation was used to obtain the Young modulus of the SWCNTs[47]

$$E_{\mathrm{CNT}} = A/r_{\mathrm{CNT}} + B \quad (4)$$

where A = 429.6 GPa nm and B = 8.42 GPa.

In our case, the CNT radius r_{CNT} is 0.7 nm, and therefore E_{CNT} = 620 GPa. It follows that the ratio of E_{CNT}/E_{PI} is large, i.e. both η_L and η_T are close to 1, and in practice only a rough estimate for E_{CNT} is needed.

With these values, eq 3 gives slightly too large values (about 15% for PI−SWCNT1) and the deviation increases with increasing CNT content. On the basis of eq 3, the experimental results for E imply an aspect ratio that stays constant at about 500 up to about 5 wt % SWCNTs (solid line in Figure 6b), and then decreases to 300 as the CNT content increases further from 5 to 20 wt %. This corresponds to an increase of CNT diameter from about 2 nm up to 3.3 nm for a CNT length of 1000 nm. That is, eq 3 can account for the experimental results if the CNTs are almost fully debunded at low CNT content, and if the bundle size increases to slightly less than the bundle size for the purchased material (4−5 nm) for composites with 20 wt % SWCNTs. This is a plausible result which agrees with the other observations made above.

Effect of the High Pressure High Temperature Treatment on the Density of the Composites. Since the HP&HT treatment induces cross-links, one can expect a concomitant irreversible increase of density. That is, the density increase at the high-pressure cross-linking transformation, which must occur according to fundamental thermodynamics,[35] probably persists in the samples recovered at room temperature. This presumption was also verified by density measurements on both pure PI and the composites. The density of the composites, before the HP&HT treatments, can be estimated by the mixture rule, which is given by

$$\rho_{composite} = \frac{1}{\frac{w_{PI}}{\rho_{PI}} + \frac{w_{\mathrm{CNT}}}{\rho_{\mathrm{CNT}}}} \quad (5)$$

where w is the weight fraction, and ρ_{PI} is the density of PI (0.92 g cm^{-3}), and ρ_{CNT} is the density of SWCNTs (1.2−1.5 g cm^{-3}, as estimated by the supplier, and the maximum value was used for the density estimates to obtain an upper limit of the density). The mixture rule predicts an almost linear, but with a slightly positive curvature, increase of density with increasing CNT content. These results are shown in Figure 6d together with the experimental results for samples treated at 513 K at 1 GPa.

For the HP&HT treated PI at 1 GPa, we find ρ_{PI} = 0.946 g cm^{-3} as an average for samples of two different batches, and this is about 3% higher than that for virgin PI. With 1 wt % CNTs, the density of the cross-linked sample increases 4% compared to that predicted by the mixture rule. We can therefore conclude that the HP&HT treatment yields densified elastomeric states, and that the irreversible HP&HT induced densification is augmented by the presence of CNTs. The latter follows from both the more pronounced density increase for the samples with CNT content and, even more convincingly, from the leveling off at high CNT contents, which is opposite to that predicted by the mixture rule. We can thus confidently ascribe the augmented densification to a change in the PI matrix caused by the CNTs. The leveling off can either be due to an increasing degree of agglomeration, but also a natural consequence of the large surface area per unit mass of the CNTs. Already at low content of SWCNTs, the distance between the polymer chains and a CNT is typically within a few tenths of a nanometer. For example, perfectly dispersed and aligned SWCNTs, give an inter CNT distance of less than ∼20 nm for a 5 wt % PI−SWCNT composite. It follows that a major part of the polymer can be affected at low CNT contents and that further increase would be less effective. Although the effect is small, it is remarkable that the weak PI−CNTs interaction increases the density of the PI matrix. Further studies are needed to explore if the same effect occurs in other polymer−CNT composite made under atmospheric pressure conditions, or if this is an effect increased to a detectable level by the high pressure treatment.

Reduction of Brittleness Induced by the Carbon Nanotubes. The tensile results show that the CNTs increased the extension at break for highly cross-linked samples up to at least 5 wt % CNTs, and the CNTs also facilitated the extraction of the samples after synthesis[32] for samples produced at 1 GPa and above. From these results, we deduce that the CNTs reduce the brittleness of the PI matrix, which is another interesting effect of the CNTs. The reason for this may be revealed by scanning electron microscopy (SEM) images of samples subjected to tensile testing. SEM images of 10 and 20 wt % PI−SWCNT composites and pure PI are shown in Figure 8. The images of the composites show a number of microcracks that has developed perpendicularly to the direction of tension, and the parts inside the cracks reveals bridges, which is a behavior different from that of pure PI, which showed very few cracks and no bridges. Also a 5 wt % composites was studied and showed bridges but with less frequency and not as clear as for the 10 wt % composite. The behavior of the composites seem similar to crazing, i.e., the bridging of microcracks by polymer fibrils when cracks develops in a polymer sample under tension. Because of the limited resolution, the bridges that can be observed here

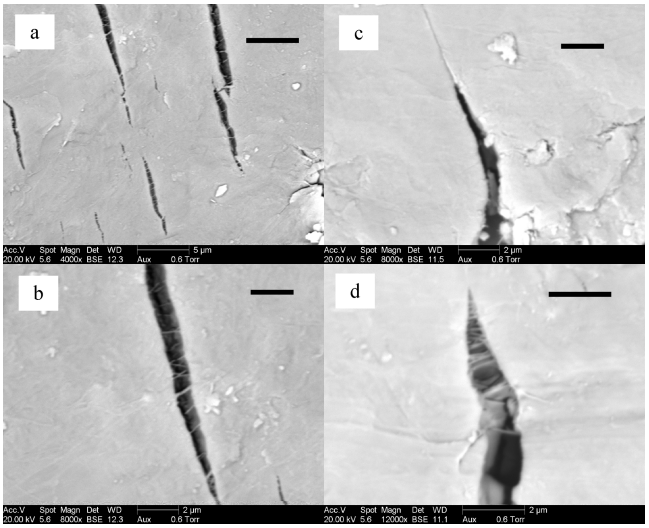

Figure 8. SEM images of samples after tensile testing: (a and b) PI−SWCNT10, (c) PI pure and (d) PI−SWCNT20. The scale bars are (a) 5 μm and (b−d) 2 μm. The samples had been covered with a gold layer of about 50 nm thickness.

are wider (ranging from a few tenth of a nanometer to about 200 nm) than normal fibrils, which have widths of order of nanometers. In this case, CNTs are required for this to occur in the highly cross-linked samples, and the CNTs probably also take part in the bridges. It seems contradictory that the CNTs both promote cross-linking and a phenomenon similar to crazing, despite that the latter should not occur in a highly cross-linked sample. But this is reconciled by our deduction that the SWCNT−PI interaction promotes mainly physical cross-links/constraints and that the CNTs act as sites for the development of the bridges of the microcracks by disrupting a continuous network of chemical cross-links in PI.

We may thus have identified two nanolevel phenomena that affect the tensile properties of the composites as the pressure of the HP&HT treatment increases: improved interfacial contact between the CNTs and the matrix, and disruption of the matrix network, which is noticeable only at high cross-link densities. The former improves the tensile strength of the composites and the latter makes these less brittle, but it also weakens the polymer matrix and the increases of the tensile strength and modulus become less prominent at high cross-link densities.

Conclusions

We have shown that liquid polyisoprene (PI) and its single wall carbon nanotube (SWCNT) composites (1−20 wt %) can be cross-linked into network polymers by high pressure treatment at 513 K in the 0.5−1.5 GPa range. The tensile strength and Young's modulus of PI increase strongly with increasing pressures for the cross-link process, with a simultaneous gradual change from elastomeric to brittle behavior. A similar behavior is shown for the tensile properties of the SWCNT composites, and a 5 wt % SWCNT composite had 2.2 times higher tensile strength and 2.3 times higher Young's modulus than those of the strongest cross-linked pure PI. These changes in the tensile properties occur simultaneously as the measured cross-link density and mass density increase, and we find that the interfacial contact between the CNTs and the PI matrix improves as a result of cross-linking a densified matrix. Another interesting observation is a CNT induced reduction of the composite brittleness despite that the composite shows a higher measured cross-link density than pure PI. This seems to originate from an effect similar or identical to crazing, i.e., bridging of microcracks by polymer fibrils. We surmise that the higher cross-link densities of the composites are due mainly to physical cross-links/constraints that limits swelling in a solvent, and that the CNTs promote material flow by disrupting an otherwise chemically cross-linked network. Moreover, the results show that the CNT−PI interfacial interaction causes an increase of the density of the polyisoprene matrix, which levels off at high CNT content. Further measurements are needed to see if this is specific for high pressure cross-linked PI−CNT composites or a general feature of polymer CNT composites.

This study has shown that cross-linking under high quasi-hydrostatic pressure can improve interfacial interaction between CNTs and a polymer matrix, and we note that high pressure cross-linking may be viable also in, e.g., extrusion processing.

Acknowledgment. This work was financially supported by SIDA/SAREC of Sweden and the Swedish Research Council.

References and Notes

(1) *Physical Properties of Polymers Handbook*, 2nd ed.; Mark, J. E., Ed. Springer-Verlag: New York, 2007.
(2) Iijima, S. *Nature* **1991**, *354*, 56–58.
(3) Garboczi, E. J.; Snyder, K. A.; Douglas, J. F.; Thorpe, M. F. *Phys. Rev. E.* **1995**, *52*, 819–828.
(4) O'Connell, M. J. *Carbon Nanotubes: Properties and applications*: CRC Press, Taylor & Francis Group: New York, 2006, 213−274.
(5) Coleman, J. N.; Khan, U.; Gun'ko, Y. K. *Adv. Mater.* **2006**, *18*, 689–706.
(6) Xie, X.-L.; Mai, Y.-W.; Zhou, X.−P. *Mater. Sci. Eng. R* **2005**, *49*, 89–112.
(7) Moniruzzaman, M.; Winey, K. I. *Macromolecules* **2006**, *39*, 5194–5205.
(8) Baughman, R. H.; Zakhidov, A. A.; de Heer, W. A. *Science* **2002**, *297*, 787–792.
(9) Thess, A.; Lee, R.; Nikolaev, P.; Dai, H. J.; Petit, P.; Robert, J.; Xu, C. H.; Lee, Y. H.; Kim, S. G.; Rinzler, A. G.; Colbert, D. T.; Scuseria, G. E.; Tomanek, D.; Fischeer, J. E.; Smalley, R. E. *Science* **1996**, *273*, 483–487.
(10) Saito, R.; Dresselhaus, G.; Dresselhaus, M. S. *Physical properties of carbon nanotubes*; London Imperial College Press: London, 1998.
(11) Awasthi, K.; Srivastava, A.; Srivastava, O. N. *J. Nanosci. Nanotechnol.* **2005**, *5*, 1616–1636.
(12) Overney, G.; Zhong, W.; Tomanek, D. *Z. Phys. D.* **1993**, *27*, 93–96.
(13) Lu, J. P. *Phys. Rev. Lett.* **1997**, *79*, 1297–1300.
(14) Blakslee, O. L.; Proctor, D. G.; Seldin, E. J.; Spence, G. B.; Weng, T. *J. Appl. Phys.* **1970**, *41*, 3373–3382. Seldin, E. J.; Nezbeda, C. W. *J. Appl. Phys.* **1970**, *41*, 3389–3400.
(15) Frank, I. W.; Tanenbaum, D. M.; Van Der Zande, A. M.; McEuen, P. L. *J. Vac. Sci. Technol. B* **2007**, *25*, 2558–2561.
(16) Van Enkevort, W. J. P. *Synthetic Diamond*; Spear, K. E., Dismukes, J. P., Eds.; Wiley: New York, 1994; p 315.
(17) Yu, M. F.; Files, B. S.; Arepalli, S.; Ruoff, R. S. *Phys. Rev. Lett.* **2000**, *84*, 5552–55.
(18) *Handbook of plastics, elastomers, and composites*, 4th ed. Harper, C. A.; McGraw-Hill: New York; 2002.
(19) Aklonis, J. J.; MacKnight, W. J. *Introduction to Polymer Viscoelasticity*; J. Wiley & Sons: New York, 1983.
(20) Wood, L. A. In *Polymer Handbook*, 3rd ed.; Brandrup, J., Immergut, E. H., Eds.; Wiley: New York, 1989; V/7.
(21) Coleman, J. N.; Khan, U.; Blau, W. J.; Gun'ko, Y. K. *Carbon* **2006**, *44*, 1624–1652.
(22) Bokobza, L. *Polymer* **2007**, *48*, 4907–4920.
(23) Bellander, M. Ph.D. Thesis, Royal Institute of Technology: Stockholm, 1998, and references therein.
(24) Kaminski, K.; Paluch, M.; Wrzalik, R.; Ziolo, J.; Bogoslovov, R.; Roland, C. M. *J Polym. Sci.; Part A: Polym Chem.* **2008**, *46*, 3795–3801.
(25) Tonpheng, B.; Andersson, O. *Eur. Polym. J.* **2008**, *44*, 2865–2873.
(26) Tonpheng, B.; Yu, J.; Andersson, O. *Macromolecules* **2009**, *42*, 9295–9301.
(27) Scheirs, J. *Compositional and Failure Analysis of Polymers: A Practical Approach*. John Wiley & Sons: Chichester, U.K., 2000.

(28) Flory, P. J.; Rehner, J., Jr. *J. Chem. Phys.* **1943**, *11*, 512–520.
(29) Flory, P. J. *J. Chem. Phys.* **1950**, *18*, 108–111.
(30) Horkay, F.; McKenna, G. B.; Deschamps, P.; Geissler, E. *Macromolecules* **2000**, *33*, 5215–5220.
(31) Tonpheng, B.; Andersson, O. *High Pressure Res.* **2006**, *26*, 415–419.
(32) The increased brittleness of the pure PI samples complicated the tensile testing as microcracks easily developed and grew when the sample was slightly bended. As a consequence, the recovery of the pure PI samples from the high-pressure sample cell occasionally failed for samples made at the highest pressures.
(33) Tonpheng, B.; Yu, J.; Andersson, O. *High Pressure Res.* **2008**, *28*, 587–590.
(34) Charlesby, A. *Radiat. Phys. Chem.* **1992**, *40*, 117–120.
(35) Considering the results of the transformation at various pressures and 513 K, then a state with cross-links must have smaller volume than one without. This follows from the thermodynamic relation that the change of Gibbs free energy G with an isothermal change in pressure p is equal to the volume V, i.e. $(\partial G/\partial p)_T = V$. The results show that the transformation does not occur at 1 bar, at least not noticeably, but proceeds to a state with increasingly more cross-links when the pressure is increased isothermally at 513 K. Consequently, G of the state without cross-links increases more than those with cross-links, and the volume of the latter must be smaller.
(36) Bellander, M.; Stenberg, B.; Persson, S. *Polym. Eng. Sci.* **1998**, *38*, 1254–1260.
(37) Bellander, M.; Stenberg, B.; Persson, S. *J. Appl. Polym. Sci.* **1999**, *73*, 2799–2806.
(38) Kuczkowski, J. A. In *Oxidation Inhibition in Organic Materials*, Pospisil, J., Klemchuk, P. P., Eds.; CRC Press Inc.: Boca Raton, FL, 1989, Vol. *I*, p 247.
(39) For one of the composites, the cross-link density was measured for pieces taken in the middle and on the side of the plate, and the results differed 20% with a higher density on the side. Thus the cross-link density may vary in the samples possibly due to pressure and/or temperature gradients.
(40) Valentín, J. L.; Mora-Barrantes, I.; Carretero-Gonzalez, J.; López-Manchado, M. A.; Sotta, P.; Long, D. R.; Saalwächter, K. *Macromolecules* **2010**, *43*, 334–346.
(41) Baskaran, D.; Mays, J. W.; Bratcher, M. S. *Chem. Mater.* **2005**, *17*, 3389–3397.
(42) Tallury, S. S.; Pasquinelli, M. A. *J. Phys. Chem. B* **2010**, *114*, 4122–4129.
(43) Agarwal, B. D.; Broutman, L. G. *Analysis and Performance of Fiber Composites*; Wiley: New York, 1980.
(44) Halpin, J. C.; Tsai, S. W. *Environmental factors in composite materials design*; US Air Force Technical Report AFML TR, 1967.
(45) Mallick, P. K. *Fiber-Reinforced Composites*; Marcel Dekker: New York, 1993.
(46) Nielsen, L. E.; Landel, R. F.; *Mechanical properties of polymers and composites*. 2nd ed. Marcel Dekker: New York, 1994.
(47) Pipes, R. B.; Frankland, S. J. V.; Hubert, P.; Saether, E. *Compos. Sci. Technol.* **2003**, *63*, 1349–1358.